Published in the Proceedings of the 4th World Congress on Emulsions, Lyon, France, 3-6 October 2006; Paper No. 2.2-377

Mechanism of Drop Detachment from Micro-Pores with Application to Membrane Emulsification

Krassimir D. Danov*, Peter A. Kralchevsky, Nikolay C. Christov, Darina K. Danova

Laboratory of Chemical Physics and Engineering, Faculty of Chemistry, University of Sofia, 1164 Sofia, Bulgaria

Abstract. We investigate theoretically and experimentally the production of monodisperse emulsions by means of microporous membranes. To understand the mechanism of drop detachment from a pore, theoretical calculations for the case without cross flow have been performed. The driving force of the drop detachment turns out to be the viscous stress due to the flow of the liquid, supplied by the pore, which feeds the growing drop. For drop detachment, it is not necessary the viscous stress to cause a violation of the force balance in the system. Instead, it is sufficient the viscous stress to produce a deformation in the drop shape, which leads to the appearance of a necking instability, in analogy with the case of a pendant drop. This instability brings about the drop detachment, which corresponds to a transition from stable to unstable equilibrium. The drag coefficients of the driving force, due to the liquid flow inside the growing drop, f_a, and of the resistance force, due to the outer fluid, f_b, are computed. The regimes of fixed transmembrane pressure and fixed flow rate are investigated. The theoretical predictions about the dependence of the emulsion drop size on various factors (interfacial tension, pore size, applied pressure, viscosities of the two liquid phases) are compared with experimental results for emulsions produced by means of Shirasu porous glass membranes.

Keywords: membrane emulsification; monodisperse emulsions; drop detachment from pores; microporous membranes; drop-size distribution.

***Corresponding author**: Krassimir D. Danov, E-mail: kd@lcpe.uni-sofia.bg

1. Introduction

The method of membrane emulsification (see Fig. 1) has found a considerable development and many applications during the last decade. This method has been applied in many fields, in which monodisperse emulsions are needed. An example is the application in food industry for production of oil-in-water (O/W) emulsions: dressings, artificial milk, cream liqueurs, as well as for preparation of some water-in-oil (W/O) emulsions: margarine and low-fat spreads. Another application of this method is for fabrication of monodisperse colloidal particles: silica-hydrogel and polymer microspheres; porous and cross-linked polymer particles; microspheres containing

carbon black for toners, etc. A third field of utilization is for obtaining multiple emulsions and microcapsules, which have found applications in pharmacy and chemotherapy. Closely related to the membrane emulsification is the method employing capillary tubes and micro-channels to produce monodisperse emulsions (1-4).

A key problem of membrane emulsification is to explain and predict the dependence of the drop diameter, $2R_d$, on the experimental parameters: pore diameter, $2R_p$, applied cross flow in the continuous phase, flux of the disperse phase along the pores, viscosity of the oil and water phases, interfacial tension, kinetics of surfactant adsorption, etc. The values of the ratio R_d/R_p, reported in different experimental works, vary in the range from 2 to 10; the reasons for this variation have not yet been well understood.

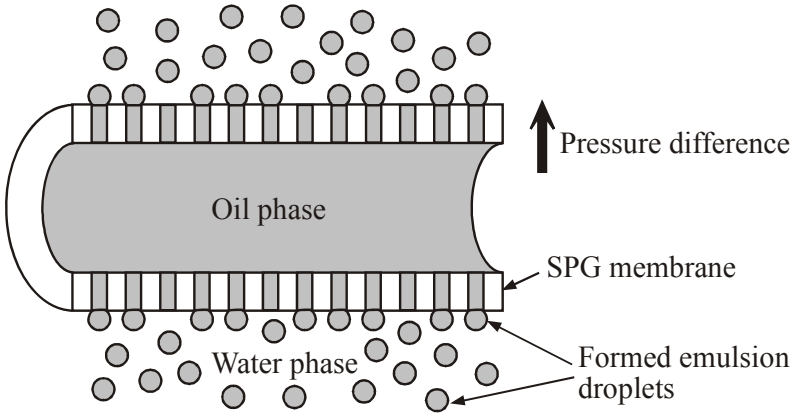

Fig. 1. Sketch of the used membrane emulsification method: the oil phase is supplied under pressure in a tubular microporous glass membrane; the emulsion drops appear at the outer surface of the membrane, which is immersed in the water phase.

Our study is aimed at revealing the hydrodynamic factors that govern the drop detachment from the orifice of a pore. As a first step, here we address the simpler case of drop formation in the *absence* of external cross-flow. Experiments with Shirasu porous glass (SPG) membranes have been carried out. Further, we solved the hydrodynamic problem in the three spatial regions: (i) inside the pore; (ii) inside the growing drop; and (iii) in the outer liquid phase. The driving force, due to the liquid flow inside the growing drop, and the resistance force, due to the outer fluid, are quantified. Our working hypothesis is that these forces cause deformation of the drop surface that leads to a necking instability and drop detachment, analogous to the instability that causes the breakage of pendant drops.

2. Experimental results

The experimental method and procedures are described in Ref. (3). Fig. 2 shows a typical experimental drop size distribution, which can be described by a Gaussian bell-like curve. In Fig. 2, one sees that $R_d/R_p \approx 3.1$. We obtain similar values in most of our experiments. For example, we varied the interfacial tension σ by one order of magnitude ($0.4 < \sigma < 4$, mN/m) by addition of NaCl to a solution of 5 mM AOT (sodium bis(2-ethylhexyl) sulfosuccinate, Sigma). For the produced drops, we obtained $R_d/R_p \approx 3$ irrespective of the value of σ. In another series of experiments, σ was fixed, but R_p was varied by using different membranes; again $R_d/R_p \approx 3$ was obtained. Moreover, the same result is obtained when the viscosity of the drop (oil) phase was increased from 2 to 50 mPa.s at fixed viscosity of the outer aqueous phase. Thus, the main question, which the theory should answer, is why $R_d/R_p \approx 3 - 3.5$ irrespective of the interfacial tension, pore size and the viscosity of the drop phase.

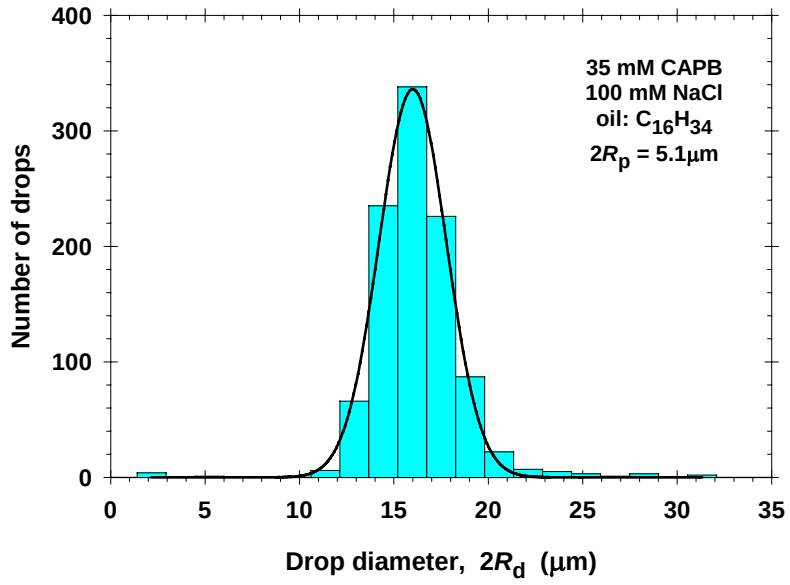

Fig. 2. Size distribution of hexadecane drops formed by membrane emulsification in 35 mM aqueous solution of cocoamidopropyl betaine (CAPB) + 100 mM NaCl. SPG membrane of pore diameter $2R_p = 5.1$ μm is used. The curve is a Gaussian fit.

3. Theoretical modeling of the drop detachment from a pore

Our working hypothesis is as follows. For drop detachment, it is sufficient the viscous stress to produce a deformation in the drop shape, which leads to the appearance of a necking instability, in analogy with the case of a pendant drop. The instability brings about the drop detachment, which corresponds to a transition from stable to unstable equilibrium.

Both the theoretical analysis and the experiment indicate that a *pendant* drop is stable up to the point of the volume maximum, V_m, and becomes unstable at this point (5,6). Harkins and Brown (7) expressed the maximum gravitational force (weight) for a pendant drop as follows:

$$F^{(g)} \equiv \Delta\rho\, g V_m = 2\pi R_p \sigma\, f_{HB} \qquad [1]$$

$\Delta\rho$ is the density difference between the two liquids; g is the gravity acceleration, and R_p is the pore radius. The Harkins-Brown factor, f_{HB}, is related to the instability of the drop profile and is independent of g. One can calculate f_{HB} from the equation:

$$f_{HB} = \frac{1}{2\pi\lambda}[V_{max}(\lambda)]^{2/3} \qquad [2]$$

where V_{max} is the dimensionless V_m. In Ref. (8), V_{max} is tabulated as a function of the dimensionless parameter $\lambda = R_p/(V_m)^{1/3}$.

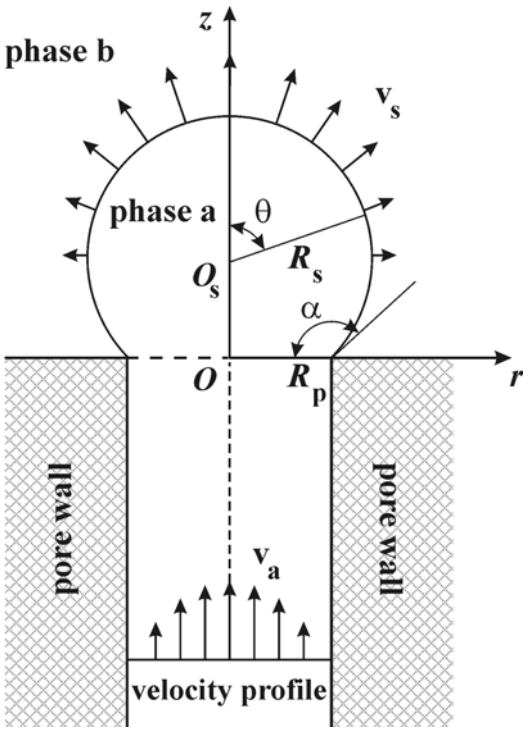

Fig. 3. Drop from the liquid phase 'a' growing at the orifice of a membrane pore. Phase 'b' is the outer liquid medium. R_p and R_s are the radii of the cylindrical pore and spherical drop surface. For a given R_p, the angle α characterizes the drop size.

In the case of membrane emulsification, the emulsion drops are so small that the gravitational deformation of their surfaces is completely negligible. However, the emulsion drops, growing at the opening of a membrane pore, can be deformed by the hydrodynamic flow of the inner phase. Then, an elongated profile, similar to that of the pendant drop, will be formed. Such elongated drop has a limit of its stability (maximum

volume, V_m) after which it becomes unstable and detaches from the pore. In analogy with Eq. [1], we make the model assumption that at the moment of detachment, the hydrodynamic force, F_h, acting on the drop is equal to the effective body force that would cause shape instability and detachment:

$$F_h = 2\pi R_p \sigma f_{HB} \qquad [3]$$

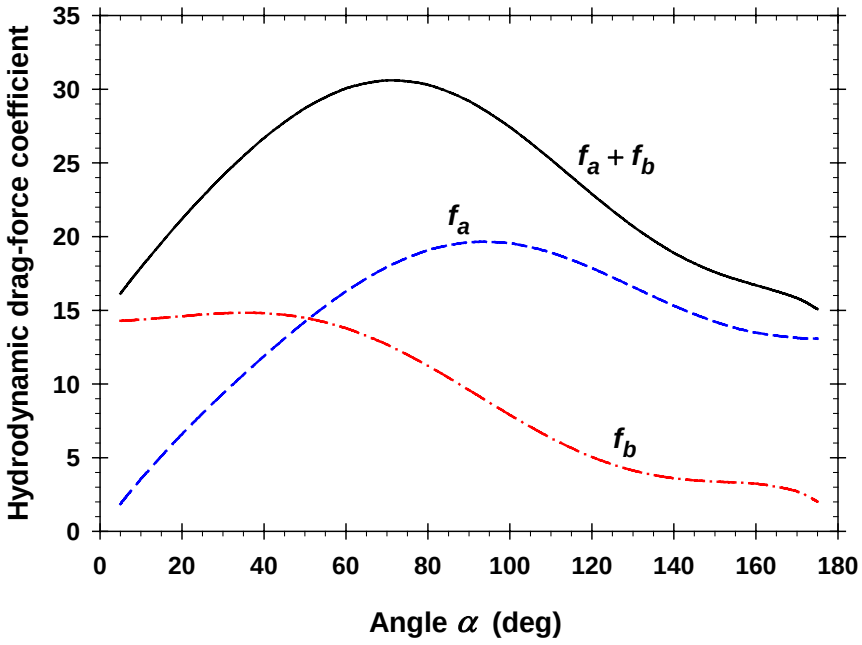

Fig. 4. Plot of the computed dimensionless drag-force coefficients $f_a(\alpha)$ and $f_b(\alpha)$ related to the hydrodynamic flow in the inner phase 'a' and outer phase 'b' (Fig. 3).

The hydrodynamic force acting on the forming emulsion drop, can be expressed in the form $F_h = f_h \eta_a R_p v_m$, where η_a is the viscosity of the inner fluid, v_m is the mean velocity of this fluid along the channels of the membrane and f_h is a hydrodynamic drag-force coefficient, which can be presented in the form:

$$f_h \equiv f_a(\alpha) + \frac{\eta_b}{\eta_a} f_b(\alpha) \qquad [4]$$

where $f_a(\alpha)$ and $f_b(\alpha)$ are plotted in Fig. 4; η_b is the viscosity of the outer fluid; α is an angle that characterizes the size of the growing drop (Fig. 3); $f_a(\alpha)$ and $f_b(\alpha)$ are contributions to f_h due to the inner and outer fluid, respectively. We solved the respective hydrodynamic problem assuming that the oil-water interface is spherical (of radius R_s) during the process of drop growth at the tip of the capillary (Fig. 3). As a result, we computed $f_a(\alpha)$ and $f_b(\alpha)$, which are dimensionless functions of α; see Fig. 4. Note that f_a and f_b depend only on α, but are independent of the other geometrical and

material parameters. Substituting $F_h = f_h \eta_a R_p v_m$ in Eq. [3] and using Eq. [2], we obtain the *condition for drop detachment* in the form:

$$f_h \eta_a v_m = \frac{\sigma}{\lambda}[V_{max}(\lambda)]^{2/3} \quad [5]$$

where $V_{max}(\lambda)$ is a universal function given by Eq. [4] in Ref. (8). Because $V_m = (4/3)\pi R_d^3$ and $\lambda = R_p/(V_m)^{1/3}$, we have:

$$\frac{R_d}{R_p} \equiv \frac{1}{R_p}\left(\frac{3V_m}{4\pi}\right)^{1/3} = \left(\frac{3}{4\pi}\right)^{1/3}\frac{1}{\lambda} \approx \frac{0.62035}{\lambda} \quad [6]$$

In addition, one could express the drop volume V_m in terms of R_p and α (Fig. 3), and using again the definition $\lambda = R_p/(V_m)^{1/3}$ we obtain:

$$\lambda^{-3} = \frac{\pi}{3}\frac{2+\cos\alpha}{(1+\cos\alpha)^2}\sin\alpha \quad [7]$$

4. Drop formation in regime of constant transmembrane pressure

This regime is realized by applying a constant pressure difference, ΔP, across the emulsification membrane. In our experiments, the pressure was supplied by a gas bottle. For a Poiseuille flow along a channel of length L, the mean velocity of the fluid, v_m, is proportional to the applied pressure difference (9):

$$v_m = \frac{R_p}{8\eta_a L}\left(\Delta P - \frac{2\sigma}{R_s}\right) \quad [8]$$

The driving pressure of the flow is smaller than the total transmembrane pressure, ΔP, because of the pressure difference, $2\sigma/R_s$, across the spherical drop surface (Fig. 3). Substituting Eq. [8] into Eq. [5], we derive the following expression for ΔP:

$$\Delta P = \frac{2\sigma}{R_p}\{4[V_{max}(\lambda)]^{2/3} l/[\lambda f_h(\alpha)] + \sin\alpha\} \quad [9]$$

Here, $l = L/R_p$, and we have used the fact that $R_s = R_p/\sin\alpha$ (Fig. 3). We recall that $V_{max}(\lambda)$ is a universal function given by Eq. [4] in Ref. (8). In Fig. 5, we have plotted ΔP versus R_d/R_p for two values of the viscosity ratio η_b/η_a. We used the following procedure of calculations. First, for a given value of α, from Eqs. [4] and [7] we determine f_h and λ. Second, from Eq. [6] we calculate R_d/R_p. Finally, from Eq. [9] we find ΔP. Because the emulsification membranes are composed of cavities connected by channels, L is typically of the order of R_p. For this reason, when calculating ΔP (Fig. 5), we substituted $l \approx 1$ in Eq. [9].

The curves in Fig. 5 exhibit minima at R_d/R_p = 3.45 and 3.60, respectively, for η_b/η_a = 0.5 and 1.0. The latter two values of R_d/R_p correspond to α = 163.1° and 163.9°. The value $\Delta P = \Delta P_{cr}$ at the minimum represents the critical transmembrane pressure for drop formation. When the applied pressure is gradually increased, the production of drops begins suddenly, at $\Delta P = \Delta P_{cr}$. If ΔP is kept slightly above ΔP_{cr}, but close to ΔP_{cr}, which is the situation in many experiments (including ours), one would obtain drops of R_d/R_p slightly below the value of R_d/R_p at the minimum (i.e. close to 3), which is experimentally observed. As illustrated in Fig. 5 (see the horizontal line with $\Delta P > \Delta P_{cr}$), the model predicts that at greater values of ΔP one produces smaller drops. In the limiting case of very high ΔP, the ratio R_d/R_p approaches 1, as observed in another series of our experiments.

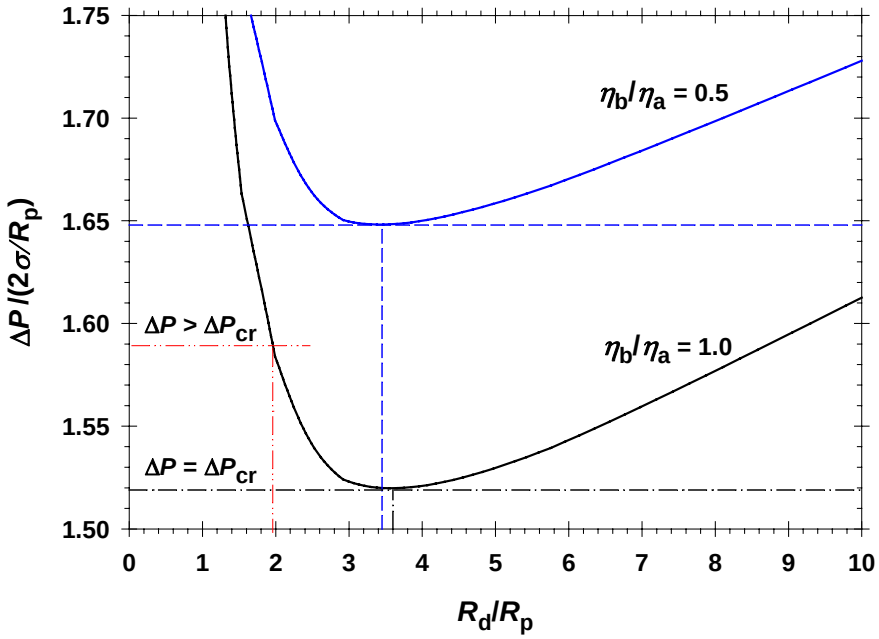

Fig. 5. The transmembrane pressure, ΔP, scaled with the capillary pressure, $2\sigma/R_p$, as a function of R_d/R_p for two values of the viscosity ratio, η_b/η_a. The minimum represents the critical pressure for drop detachment, ΔP_{cr}. For a given $\Delta P > \Delta P_{cr}$, the intersection point of the respective horizontal line with the left branch of the calculated curve determines the dimensionless radius, R_d/R_p, of the formed drops.

The viscosity of the drop phase, η_a, cancels when we combine Eqs. [5] and [8] to derive Eq. [9]. Consequently, in the considered regime (of constant transmembrane pressure) the effect of viscosity comes only through the ratio η_b/η_a in Eq. [4]. For $\eta_b/\eta_a < 1$, the respective term in Eq. [4] becomes negligible, and the value of R_d/R_p at the minimum approaches 3.25 for $\eta_b/\eta_a = 0$. In contrast, for $\eta_b/\eta_a > 1$, the respective term in Eq. [4] becomes considerable, which leads to the detachment of larger drops at higher

viscosities of the outer phase. This is what we observe experimentally when we dissolve greater amounts of glycerol to increase the viscosity of the outer (aqueous) phase.

5. Drop formation in regime of constant flow rate

Experimentally, this regime could be realized when the disperse phase is supplied with a constant speed by a pump. Then, the mean velocity of the liquid in the capillary channel is:

$$v_{\rm m} = \frac{V_{\rm m}}{\pi R_{\rm p}^2 t_{\rm d}} = \frac{R_{\rm p}}{\pi \lambda^3 t_{\rm d}} \qquad [10]$$

where $t_{\rm d}$ is the period of drop formation and we have used the definition $\lambda = R_{\rm p}/(V_{\rm m})^{1/3}$. Substituting Eq. [10] into Eq. [5], we derive:

$$\frac{1}{\tau} \equiv \frac{\eta_{\rm a} R_{\rm p}}{\sigma t_{\rm d}} = \frac{\pi \lambda^2}{f_{\rm h}(\alpha)} [V_{\rm max}(\lambda)]^{2/3} \qquad [11]$$

where τ is the dimensionless period of drop formation; $V_{\rm max}(\lambda)$ is a universal function given by Eq. [4] in Ref. (8). Thus, one could determine the dependence of the relative size of the detached drops, $R_{\rm d}/R_{\rm p}$, on the period of drop formation, $t_{\rm d}$, in regime of constant flow rate. The computational procedure is the following. First, for a given value of α, and for a fixed ratio $\eta_{\rm b}/\eta_{\rm a}$, from Eqs. [4] and [7] we determine $f_{\rm h}$ and λ. Second, from Eq. [6] we calculate and $R_{\rm d}/R_{\rm p}$. Finally, from Eq. [11] we find $t_{\rm d}$. The obtained results indicate that the relative drop size, $R_{\rm d}/R_{\rm p}$, decreases with the increase of the frequency of drop release, $1/t_{\rm d}$. In this regime, the effect of the viscosity of the inner fluid, $\eta_{\rm a}$, is considerable because of the multiplier $\eta_{\rm a}$ in Eq. [11].

6. Conclusions

To understand the mechanism of drop detachment from a pore, theoretical calculations have been performed, which gave the dependence of the hydrodynamic drag-force coefficient, $f_{\rm h}$, on the drop size; see Eq. [4] and Fig. 4. Assuming that the viscous stresses produce a deformation in the drop shape, which leads to the appearance of a necking instability and drop breakage, we derived a condition for drop detachment, Eq. [5]. In regime of emulsification under constant transmembrane pressure, we derived a relation between $R_{\rm d}/R_{\rm p}$ and the applied pressure, ΔP; see Eq. [9]. It predicts that the plot of ΔP vs. $R_{\rm d}/R_{\rm p}$ exhibits a minimum at $R_{\rm d}/R_{\rm p} \approx 3.5$ (Fig. 5), which corresponds to the critical pressure for drop detachment, $\Delta P = \Delta P_{\rm cr}$. In the experiment one often works at

ΔP slightly above ΔP_{cr}, but close to ΔP_{cr}, which corresponds to $R_d/R_p \approx 3$. The theory predicts that value of R_d/R_p at the minimum is insensitive to the interfacial tension, σ, pore radius, R_p, and on the viscosity ratio, η_b/η_a (if $\eta_b/\eta_a < 1$). For $\eta_b/\eta_a > 1$, the increase of η_b/η_a leads to the formation of bigger drops (greater R_d/R_p). These theoretical predictions are in agreement with our experimental observations (Section 2). Similar analysis can be applied to the case of emulsification under constant flow rate (Section 5). Additional work is necessary to complete the comparison of theory and experiment with respect to the influence of the various factors.

Acknowledgments. We gratefully acknowledge the support of the Bulgarian NSF Program "Development of Scientific Infrastructure", and of the Program CONEX of the Austrian Ministry of Education, Science and Culture. We thank Ms. Mariana Paraskova for her assistance in the manuscript preparation.

References

1. V. Schröder, H. Schubert, *Colloids Surf. A*, 152 (1999) 103-109.
2. S.M. Joscelyne, G. Trägårdh, *J. Membrane Sci*. 169 (2000) 107-117.
3. N.C. Christov, D.N. Ganchev, N.D. Vassileva, N.D. Denkov, K.D. Danov, P.A. Kralchevsky, *Colloids Surf. A,* 209 (2002) 83-104.
4. G.T. Vladisavljević, R.A. Williams, *Adv. Colloid Interface Sci*. 113 (2005) 1-20.
5. E. Pitts, *J. Inst. Maths Applics* 17 (1976) 387-397.
6. D.H. Michael, P.G. Williams, *Proc. R. Soc. London A,* 351 (1976) 117-128.
7. W.D. Harkins, F.E. Brown, *J. Am. Chem. Soc*. 41 (1919) 499-524.
8. B. Pu, D. Chen, *J. Colloid Interface Sci.* 235 (2001) 265-272.
9. L.D. Landau, E.M. Lifshitz, *Fluid Mechanics*, Pergamon Press, New York, 1959.